PROCEEDINGS OF SCIENCE

Constraining new physics with hyperon decays

German Valencia*

School of Physics and Astronomy, Monash University,
Wellington Road, Clayton, VIC-3800, Australia

E-mail: german.valencia@monash.edu

Motivated by the LHCb and BESIII hyperon programs we discuss different possibilities to constrain new physics with rare hyperon decay modes, including the rare mode $\Sigma^+ \to p\mu^+\mu^-$, charged lepton flavour violating modes, and $\Delta S = 2$ modes. We review the status of standard model calculations of the processes that are allowed and illustrate the new physics windows that remain after considering the constraints that exist from kaon physics.

Corfu Summer Institute 2023 "School and Workshops on Elementary Particle Physics and Gravity" (CORFU2023)
27 August - 1 October 2023
Corfu, Greece

*Speaker

PoS(CORFU2023)078

1. Introduction

In recent years there has been renewed interest in the study of rare and forbidden hyperon decays. This is driven by new experiments actively studying such decays. For example, the BESIII collaboration has obtained new limits on $|\Delta S| = 2$ decays [1] and has performed a more precise measurement of $\Sigma^+ \to p\gamma$ [2]. The LHCb collaboration has measured the rate of $\Sigma^+ \to p\mu^+\mu^-$ [3] and expects to increase the precision of their result with a sample of a few hundred events that will also allow them to improve the measurement of the dimuon spectrum. The LHCb collaboration also expects to reach a sensitivity of $O(10^{-9}) - O(10^{-10})$ to $|\Delta S| = 2$ Ξ decay [4, 5] whereas BESIII expects to collect samples of $O(10^6) - O(10^8)$ Λ, Ξ and Ω baryons and be able to reach branching ratio sensitivities at the $O(10^{-5})$ level [6]. Later on, the super tau-charm factory is expected to obtain much larger samples of hyperons [7].

In this talk, we will cover three topics: the decay $\Sigma^+ \to p\mu^+\mu^-$; tests of charge lepton flavour violation (CLFV) in hyperon decay; and $|\Delta S| = 2$ modes. There is also much ongoing and expected activity concerning CP violation in hyperon decay at BESIII which we do not discuss here.

2. χPT at leading order

The matrix elements necessary for the calculation of rare semileptonic and CLFV decays of the form $B_i \to B_j \ell^+\ell^-$ can all be obtained from the chiral Lagrangian

$$\mathcal{L}_s = \frac{f_\pi^2}{4}\mathrm{Tr}\left(\partial_\mu U \partial^\mu U^\dagger\right) + \mathrm{Tr}\overline{B}(i\not{\partial} - M)B + i\mathrm{Tr}\overline{B}\gamma^\mu\left[V_\mu, B\right] \tag{1}$$

$$+\mathrm{Tr}\left(D\overline{B}\gamma^\alpha\gamma_5\{\mathcal{A}_\alpha, B\} + F\overline{B}\gamma^\alpha\gamma_5[\mathcal{A}_\alpha, B]\right) \tag{2}$$

$$+\epsilon_{kln}C\left[\left(\overline{T}_{nvw}\right)^\alpha(\mathcal{A}_{wl})_\alpha B_{vk} + \overline{B}_{kv}(\mathcal{A}_{lw})_\alpha(T_{nvw})^\alpha\right], \tag{3}$$

where $\xi = e^{i\phi/f}$, $U = \xi^2$, $A_\mu = i(\xi\partial_\mu\xi^\dagger - \xi^\dagger\partial_\mu\xi)$, $\hat{\kappa} = (\lambda_6 + i\lambda_7)/2$. The pseudoscalar meson, the baryon octet and the baryon decuplet fields are, explicitly:

$$\phi = \frac{1}{\sqrt{2}}\begin{pmatrix} \frac{1}{\sqrt{2}}\pi^0 + \frac{1}{\sqrt{6}}\eta_8 & \pi^+ & K^+ \\ \pi^- & \frac{-1}{\sqrt{2}}\pi^0 + \frac{1}{\sqrt{6}}\eta_8 & K^0 \\ K^- & \bar{K}^0 & \frac{-2}{\sqrt{6}}\eta_8 \end{pmatrix}, \; B = \begin{pmatrix} \frac{1}{\sqrt{2}}\Sigma^0 + \frac{1}{\sqrt{6}}\Lambda & \Sigma^+ & p \\ \Sigma^- & \frac{-1}{\sqrt{2}}\Sigma^0 + \frac{1}{\sqrt{6}}\Lambda & n \\ \Xi^- & \Xi^0 & \frac{-2}{\sqrt{6}}\Lambda \end{pmatrix}, \tag{4}$$

and

$$\begin{gathered} T_{111} = \Delta^{++}, \quad T_{112} = \frac{1}{\sqrt{3}}\Delta^+, T_{122} = \frac{1}{\sqrt{3}}\Delta^0, T_{222} = \Delta^-, \\ T_{113} = \frac{1}{\sqrt{3}}\Sigma^{*+}, T_{123} = \frac{1}{\sqrt{6}}\Sigma^{*0}, T_{223} = \frac{1}{\sqrt{3}}\Sigma^{*-}, \\ T_{133} = \frac{1}{\sqrt{3}}\Xi^{*0}, T_{233} = \frac{1}{\sqrt{3}}\Xi^{*-}, T_{333} = \Omega^-. \end{gathered} \tag{5}$$

Following standard methods in the literature one extracts from this Lagrangian a correspondence between quark densities or currents and hadronic transitions [8, 9], the relevant ones for this

discussion are

$$\bar{d}\gamma_\eta s \;\Leftrightarrow\; -\sqrt{\frac{3}{2}}\,\overline{n}\gamma_\eta\Lambda - \overline{p}\gamma_\eta\Sigma^+ + \sqrt{\frac{3}{2}}\,\overline{\Lambda}\gamma_\eta\Xi^0 - \frac{1}{\sqrt{2}}\,\overline{\Sigma^0}\gamma_\eta\Xi^0 + \overline{\Sigma^-}\gamma_\eta\Xi^- + i\left(\pi^+\,\partial_\eta K^- - K^-\,\partial_\eta\pi^+\right) - \frac{i}{\sqrt{2}}\left(\pi^0\,\partial_\eta\overline{K}^0 - \overline{K}^0\,\partial_\eta\pi^0\right) + \cdots, \tag{6}$$

$$\bar{d}\gamma_\eta\gamma_5 s \;\Leftrightarrow\; \frac{-D-3F}{\sqrt{6}}\,\overline{n}\gamma_\eta\gamma_5\Lambda + (D-F)\,\overline{p}\gamma_\eta\gamma_5\Sigma^+ - \frac{D-3F}{\sqrt{6}}\,\overline{\Lambda}\gamma_\eta\gamma_5\Xi^0 - \frac{D+F}{\sqrt{2}}\,\overline{\Sigma^0}\gamma_\eta\gamma_5\Xi^0 + (D+F)\,\overline{\Sigma^-}\gamma_\eta\gamma_5\Xi^- + C\,\overline{\Xi^-}\,\Omega^-_\eta + \sqrt{2}\,f\,\partial_\eta\overline{K}^0 + \cdots, \tag{7}$$

$$\bar{d}\gamma_5 s \;\Leftrightarrow\; i\sqrt{2}\,B_0\,f\overline{K}^0 + \cdots. \tag{8}$$

In addition, there are contributions from kaon poles that arise at the same order, including the following terms

$$\bar{d}\gamma_5 s \Leftrightarrow \frac{B_0}{m_K^2 - q^2}\left(\frac{-D-3F}{\sqrt{6}}(m_\Lambda + m_N)\,\overline{n}\gamma_5\Lambda + (D-F)(m_\Sigma + m_N)\,\overline{p}\gamma_5\Sigma^+ - \frac{D-3F}{\sqrt{6}}(m_\Lambda + m_\Xi)\,\overline{\Lambda}\gamma_5\Xi^0 - \frac{D+F}{\sqrt{2}}(m_\Sigma + m_\Xi)\,\overline{\Sigma^0}\gamma_5\Xi^0 + (D+F)(m_\Sigma + m_\Xi)\,\overline{\Sigma^-}\gamma_5\Xi^-\right)\cdots, \tag{9}$$

and terms involving Ω which can be found in [10].

The couplings D and F are extracted from fits to hyperon semileptonic decay while C is extracted from a fit to strong $TB\phi$ decay. Using data from [11], we find the values $D = 0.81(1)$, $F = 0.47(1)$, $C = -1.7(3)$[12]. As shown many years ago [13], if the decuplet field is included in the Lagrangian, chiral corrections to the axial octet currents are less than 30% (there are a few exceptions, $\Sigma \to n$ and $\Lambda \to \pi$, which do not appear in this discussion). It is customary to include some higher order corrections via pole form factors as in [14], for example.

The non-leptonic weak transitions between baryons are dominated by an interaction that transforms as an $(8_L, 1_R)$ under chiral rotations and can be obtained at leading order in χPT from the Lagrangian

$$\mathcal{L}^{sm}_{\Delta S=1} \;\supset\; \mathrm{Tr}\left(h_D\,\overline{B}\{\xi^\dagger\hat{\kappa}\xi, B\} + h_F\,\overline{B}\,[\xi^\dagger\hat{\kappa}\xi, B]\right) + h_C\,\left(\overline{T}_{kln}\right)^\eta\,\left(\xi^\dagger\hat{\kappa}\xi\right)_{no}\,(T_{klo})_\eta. \tag{10}$$

The couplings h_D, h_F, h_C are extracted from fits to nonleptonic hyperon decay and suffer from the well-known S/P wave problem: if the S-waves are fit, the P waves are poorly explained and vice versa. Although the reasons are understood in χPT [13], a fit to data beyond the leading order is not useful. For numerical purposes, we use the values obtained from a recent fit to S-waves, $h_D = -1.69$, $h_F = 3.96$, $h_C = 3.75$. These numbers and the full covariance matrix from the fit can be found in [12]. Unlike the semileptonic transitions which can be predicted to within 30%, we regard the value of matrix elements obtained from Eq. 10 as an order of magnitude estimate.

3. $\Sigma^+ \to p\mu^+\mu^-$

Interest in this mode peaked in 2005 when the HyperCP collaboration first measured its rate. Although their measurement, $\mathcal{B}(\Sigma^+ \to p\mu^+\mu^-) = (8.6^{+6.6}_{-5.4} \pm 5.5) \times 10^{-8}$ [15], was in agreement with SM predictions [16] the three events observed clustered near a single dimuon invariant mass, 214.3 MeV. This gave rise to speculation of a possible new particle, that is now mostly ruled out by measurements in the kaon sector. The more recent LHCb result, on the other hand, shows no bumps in the spectrum and matches well with the distribution expected from phase space [3]. A more precise determination of this dimuon mass distribution is expected from the next analysis. The interest in this mode from the perspective of new physics remains, motivated in part by the persistent anomalies in modes originating from a $b \to s\mu^+\mu^-$ quark transition.

Within the SM, $\Sigma^+ \to p\mu^+\mu^-$ is dominated by long-distance physics. The diagram in the left panel of Figure 1 illustrates how this process proceeds through photon exchange and how the associated long-distance contributions can be estimated. The shaded oval represents the weak $\Sigma \to p\gamma^*$ transition, which can be parametrized with four complex form-factors $a(q^2), b(q^2), c(q^2)$ and $d(q^2)$,

$$\mathcal{M}^{\rm LD}_{\rm SM} = \frac{-ie^2 G_{\rm F}}{q^2}\,\bar{u}_p(a+b\gamma_5)\sigma_{\kappa\nu}q^\kappa u_\Sigma\,\bar{u}_\mu\gamma^\nu v_{\bar{\mu}} - e^2 G_{\rm F}\,\bar{u}_p\gamma_\kappa(c+d\gamma_5)u_\Sigma\,\bar{u}_\mu\gamma^\kappa v_{\bar{\mu}}. \tag{11}$$

The imaginary part of these form factors can be calculated as depicted schematically on the right panel, where the $\Sigma^+ \to N\pi$ vertices are extracted from experiment and the $N\pi \to p\gamma$ scattering is obtained from leading order χPT. Furthermore, the real part of two of these form factors evaluated at zero momentum transfer, $a(0)$ and $b(0)$, can be extracted from measurements of $\Sigma^+ \to p\gamma$ (the most recent one being [2]) up to a four-fold ambiguity, and the real part of $c(q^2)$ and $d(q^2)$, as well as the momentum dependence of a and b, can be inferred using pole models [16–22]. The most recent calculation of these numbers using relativistic χPT, along with the resulting predictions for $\Sigma^+ \to p\mu^+\mu^-$, is displayed in Table 1 [23]. The Table also shows the same branching fraction omitting the real parts of the form factors c and d which are the most model-dependent. It also shows the integrated forward-backward asymmetry and the rate for $\Sigma^+ \to pe^+e^-$ that follow for each of the four solutions to Re (a) and Re (b). The corresponding results when using heavy baryon χPT instead are similar and presented in [21, 23]. There are ongoing efforts to calculate this LD amplitudes in lattice QCD [24]. The forward-backward asymmetry quoted in Table 1 corresponds to the definition

$$\tilde{A}_{\rm FB} = \frac{1}{\Gamma(\Sigma^+ \to p\mu^+\mu^-)}\int dq^2\left(\int_0^1 \frac{d^2\Gamma}{dq^2 d\cos\theta}d\theta - \int_{-1}^0 \frac{d^2\Gamma}{dq^2 d\cos\theta}d\theta\right), \tag{12}$$

where the normalisation is the rate calculated for each solution to the LD form factors, corresponding to the different rates shown in the Table. In [21] we proposed using the difference between the relativistic and heavy baryon calculations as an estimate for the theoretical uncertainty. To illustrate this, we allow the Im$(a(0))$ and Im$(b(0))$ to vary between the two values obtained with these two methods. In Figure 3 we show the resulting error in the branching fraction for each of the four solutions as a function of the ranges in parameters obtained in this fashion.

We also note that the SM short distance contribution to this mode is significantly smaller, producing a branching ratio $\mathcal{B}_{SD}(\Sigma^+ \to p\mu^+\mu^-) \sim O(10^{-12})$ or four orders of magnitude below

Re(a)MeV	Re(b)MeV	$10^8\mathcal{B}$	$10^8\mathcal{B}_{\mathrm{Re}(c,d)=0}$	$10^5\tilde{A}_{FB}$	$10^6\mathcal{B}_{ee}$
-12.14 ± 0.24	4.75 ± 0.42	2.72 ± 0.21	1.84 ± 0.15	-1.58 ± 0.04	7.6 ± 0.3
-4.75 ± 0.42	12.14 ± 0.24	7.82 ± 0.24	5.87 ± 0.22	-0.32 ± 0.02	8.3 ± 0.3
4.75 ± 0.42	-12.14 ± 0.24	4.13 ± 0.17	5.78 ± 0.22	0.91 ± 0.04	7.8 ± 0.3
12.14 ± 0.24	-4.75 ± 0.42	1.24 ± 0.09	1.80 ± 0.14	4.52 ± 0.08	7.4 ± 0.3

Table 1: Four possible values of Re($a(0)$), Re($b(0)$) and corresponding branching ratios and asymmetry for $\Sigma^+ \to p\mu^+\mu^-$. The column labelled $\mathcal{B}$ includes contributions from the four form factors, with the quoted error including only the experimental errors that propagate to the extractions of Re(a, b) andIm(a, b). The next column does not include the real parts of c and d, which are obtained from a pole model. The last column is the corresponding branching ratio for the mode $\Sigma^+ \to pe^+e^-$.

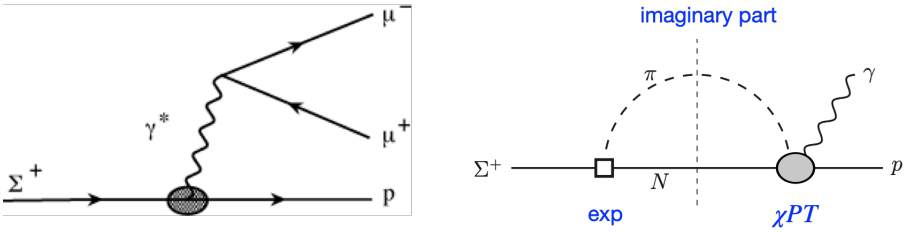

Figure 1: Left panel: long distance photon exchange contribution to $\Sigma^+ \to p\mu^+\mu^-$. The shaded oval represents the weak $\Sigma \to p\gamma^*$ transition. Right panel: cut giving rise to Im$(a(0))$ and Im$(b(0))$.

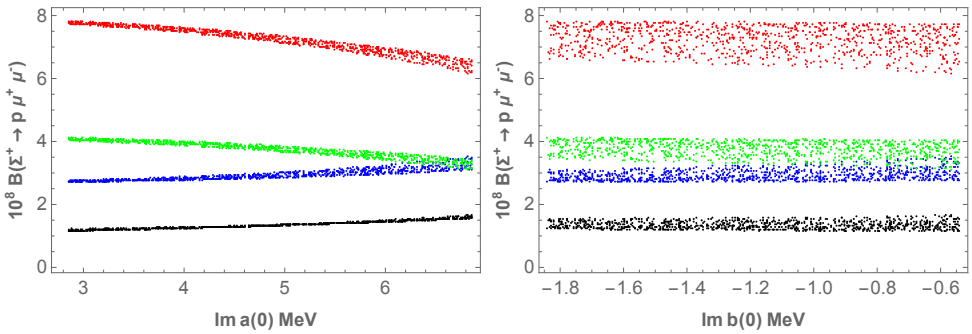

Figure 2: Branching ratio for the four solutions when the imaginary parts are allowed to range between those determined with relativistic and heavy baryon χPT.

the long distance one. Given this, constraining new physics with this mode is restricted to scenarios where the NP can enter at a level similar to that of the long-distance contributions. As briefly discussed in [21] and elaborated in [23], there are constraints complementary to those from kaon physics that can be obtained and that still allow this possibility. To study the effect of NP we consider the effective Hamiltonian

$$\mathcal{L}_{\mathrm{eff}} = -\mathcal{H}_{\mathrm{eff}} = \sum_i C_i O_i + \mathrm{H.c.}, \tag{13}$$

with operators defined as

$$O_7 = \frac{G_F}{\sqrt{2}} V_{td}^* V_{ts} \frac{e}{4\pi^2} m_s \overline{d_L} \sigma^{\kappa\nu} s_R F_{\kappa\nu}\,, \qquad O_{7'} = \frac{G_F}{\sqrt{2}} V_{td}^* V_{ts} \frac{e}{4\pi^2} m_s \overline{d_R} \sigma^{\kappa\nu} s_L F_{\kappa\nu}\,, \tag{14}$$

$$O_9^\mu = \frac{G_F}{\sqrt{2}} V_{td}^* V_{ts} \frac{e^2}{4\pi^2} \overline{d_L} \gamma^\nu s_L \overline{\mu} \gamma_\nu \mu\,, \qquad O_{9'}^\mu = \frac{G_F}{\sqrt{2}} V_{td}^* V_{ts} \frac{e^2}{4\pi^2} \overline{d_R} \gamma^\nu s_R \overline{\mu} \gamma_\nu \mu\,, \tag{15}$$

$$O_{10}^\mu = \frac{G_F}{\sqrt{2}} V_{td}^* V_{ts} \frac{e^2}{4\pi^2} \overline{d_L} \gamma^\nu s_L \overline{\mu} \gamma_\nu \gamma_5 \mu\,, \qquad O_{10'}^\mu = \frac{G_F}{\sqrt{2}} V_{td}^* V_{ts} \frac{e^2}{4\pi^2} \overline{d_R} \gamma^\nu s_R \overline{\mu} \gamma_\nu \gamma_5 \mu\,, \tag{16}$$

$$O_S = \frac{G_F}{\sqrt{2}} V_{td}^* V_{ts} \frac{e^2}{4\pi^2} m_s \overline{d_L} s_R \overline{\mu} \mu\,, \qquad O_{S'} = \frac{G_F}{\sqrt{2}} V_{td}^* V_{ts} \frac{e^2}{4\pi^2} m_s \overline{d_R} s_L \overline{\mu} \mu\,, \tag{17}$$

$$O_P = \frac{G_F}{\sqrt{2}} V_{td}^* V_{ts} \frac{e^2}{4\pi^2} m_s \overline{d_L} s_R \overline{\mu} \gamma_5 \mu\,, \qquad O_{P'} = \frac{G_F}{\sqrt{2}} V_{td}^* V_{ts} \frac{e^2}{4\pi^2} m_s \overline{d_R} s_L \overline{\mu} \gamma_5 \mu\,, \tag{18}$$

These operators also contribute to kaon decays and have been studied in the context of (although with varying notation) $K_{S,L} \to \mu^+\mu^-$ [25, 26], $K_L \to \pi^0\mu^+\mu^-$ [27–30], $K \to \pi\pi\gamma, K \to \gamma\gamma$ [31, 32], $K^+ \to \pi^+\mu^+\mu^-$ [33]. Similarly to their hyperon decay counterpart, these kaon modes receive substantial and in some cases dominant long-distance contributions. Nevertheless, certain constraints on NP emerge leaving blind directions in parameter space that can be covered by $\Sigma^+ \to p\mu^+\mu^-$ [23]. In particular, the kaon modes are only sensitive to either parity conserving or parity violating NP whereas the hyperon decay is sensitive to both. An obvious possibility to avoid kaon bounds is to choose $C_{10} = -C_{10'}$ and $C_P = -C_{P'}$ to obtain an operator proportional to $\overline{d}\gamma^\mu\gamma^5 s$ and one proportional to $\overline{d}\gamma^5 s$. If the NP is CP conserving, this operator will then only affect $K_L \to \mu^+\mu^-$ and $\Sigma^+ \to p\mu^+\mu^-$ and there is only one combination which enters $K_L \to \mu^+\mu^-$ as discussed in [23]. To fully cover the parameter space kaon constraints do not suffice. For example, for the parameter combinations C_{9-} and C_{10-} (defined as $C_{9,10} - C_{9',10'}$) we find that the tightest bounds arise from $\Sigma \to p\mu^+\mu^-$. The results are depicted in the right panel of Figure 3, where we see their allowed values can reach the 10^4 range. The four contours shown correspond to the four different SM LD solutions added to the NP contributions. Although these numbers are very large at face value, we see that they enter the effective Hamiltonian accompanied by a very strong CKM suppression, $V_{td}^* V_{ts}$. This implies that coefficients of this magnitude could appear in models without the mixing angle suppression implied by the normalization adopted in Eq. 18.

In [21], several additional observables were discussed as possible tests for NP. The forward-backward asymmetry (tabulated above) is very small in the SM, $-1.4 \lesssim \tilde{A}_{FB} \times 10^5 \lesssim 0.6$, but can reach the 5% level for certain parameter values while the branching ratio remains within the LHCb range. If the muon polarization can be measured, there are additional observables sensitive to NP also discussed in [21].

With sufficient statistics, a measurement of the dimuon spectrum can also help understand the long-distance contributions. In Figure 3 we superimpose the spectrum predicted by χPT (orange) (with a spread spanning the four solutions) on the LHCb data and the phase space model used in their analysis [3]. These measurements are also motivating lattice studies [24].

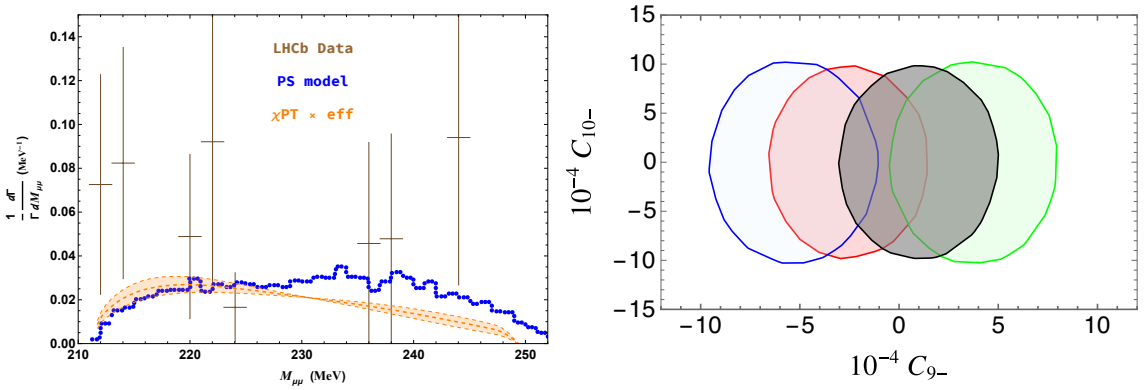

Figure 3: Left panel: range of predictions for the dimuon mass distribution from χPT compared to the LHCb measurement and the phase space spectrum (blue line). Right panel: parameter space allowed in $C_{9-} - C_{10-}$ plane.

4. CLFV hyperon decay modes

Decays exhibiting charged lepton flavour violation are sensitive probes of physics beyond the SM. In the case of hyperon decay, the modes are complementary to kaon modes and we illustrate this with a few examples. We parametrize the NP at the low scale with the same Hamiltonian as in Eq. 13 replacing the lepton bilinears $\overline{\mu}\cdots\mu$ with $\overline{\ell}\cdots\ell'$. With leptoquark exchange models in mind, we match this to the dimension six SMEFT

$$\mathcal{L}_{\rm NP} = \frac{1}{\Lambda_{\rm NP}^2}\left(\sum_{k=1}^{5} c_k^{ijxy} Q_k^{ijxy} + (c_6^{ijxy} Q_6^{ijxy} + \text{H.c.})\right) \tag{19}$$

$$Q_1^{ijxy} = \overline{q_i}\gamma^\eta q_j\, \overline{l_x}\gamma_\eta l_y \quad Q_2^{ijxy} = \overline{q_i}\gamma^\eta \tau_I q_j\, \overline{l_x}\gamma_\eta \tau_I l_y \quad Q_3^{ijxy} = \overline{d_i}\gamma^\eta d_j\, \overline{e_x}\gamma_\eta e_y$$
$$Q_4^{ijxy} = \overline{d_i}\gamma^\eta d_j\, \overline{l_x}\gamma_\eta l_y \quad Q_5^{ijxy} = \overline{q_i}\gamma^\eta q_j\, \overline{e_x}\gamma_\eta e_y \quad Q_6^{ijxy} = \overline{l_i} e_j\, \overline{d_x} q_y$$

To calculate the hyperon decay amplitude it is convenient to group the new coefficients as they appear multiplying the vector (axial vector) currents or scalar (pseudoscalar) densities:

$$\mathcal{L}_{NP} \supset \frac{-1}{\Lambda_{NP}^2}\sum_{\ell,\ell'}\Big[\overline{d}\gamma^\kappa s\,\overline{\ell}\gamma_\kappa(V_{\ell\ell'}+\gamma_5 A_{\ell\ell'})\ell' + \overline{d}\gamma^\kappa\gamma_5 s\,\overline{\ell}\gamma_\kappa(\tilde{V}_{\ell\ell'}+\gamma_5\tilde{A}_{\ell\ell'})\ell'$$
$$+\ \overline{d}s\,\overline{\ell}(S_{\ell\ell'}+\gamma_5 P_{\ell\ell'})\ell' + \overline{d}\gamma_5 s\,\overline{\ell}(\tilde{S}_{\ell\ell'}+\gamma_5\tilde{P}_{\ell\ell'})\ell'\Big]$$
$$4V_{\ell\ell'} = -c_1^{\ell\ell'} - c_2^{\ell\ell'} - c_3^{\ell\ell'} - c_4^{\ell\ell'} - c_5^{\ell\ell'}, \quad 4A_{\ell\ell'} = c_1^{\ell\ell'} + c_2^{\ell\ell'} - c_3^{\ell\ell'} + c_4^{\ell\ell'} - c_5^{\ell\ell'},$$
$$4\tilde{V}_{\ell\ell'} = c_1^{\ell\ell'} + c_2^{\ell\ell'} - c_3^{\ell\ell'} - c_4^{\ell\ell'} + c_5^{\ell\ell'}, \quad 4\tilde{A}_{\ell\ell'} = -c_1^{\ell\ell'} - c_2^{\ell\ell'} - c_3^{\ell\ell'} + c_4^{\ell\ell'} + c_5^{\ell\ell'},$$
$$4S_{\ell\ell'} = -c_6^{\ell\ell'} - c_{6'}^{\ell\ell'} = -4\tilde{P}_{\ell\ell'}, \quad 4P_{\ell\ell'} = -c_6^{\ell\ell'} + c_{6'}^{\ell\ell'} = -4\tilde{S}_{\ell\ell'}. \tag{20}$$

It is then straightforward to use the results in Eq. 6 to obtain, for example,

$$\begin{aligned}
\mathcal{B}\left(\Xi^0 \to \Lambda e^- \mu^+\right) &= \Big[2.4\left(|V_{e\mu}|^2+|A_{e\mu}|^2\right)+7.5\left(|S_{e\mu}|^2+|P_{e\mu}|^2\right)\\
&\quad +6.5\ \mathrm{Re}\left(A^*_{e\mu}P_{e\mu}-V^*_{e\mu}S_{e\mu}\right)+0.25\left(|\tilde{V}_{e\mu}|^2+|\tilde{A}_{e\mu}|^2\right)+0.07\left(|\tilde{S}_{e\mu}|^2+|\tilde{P}_{e\mu}|^2\right)\\
&\quad -0.08\ \mathrm{Re}\left(\tilde{A}^*_{e\mu}\tilde{P}_{e\mu}-\tilde{V}^*_{e\mu}\tilde{S}_{e\mu}\right)\Big]\times 10^{-5}\left(\frac{1\ \mathrm{TeV}^4}{\Lambda_{NP}}\right)^4\\
\mathcal{B}\left(K_L \to e^\pm\mu^\mp\right) &= 3.8\left[|\tilde{V}_{e\mu}+\tilde{V}^*_{\mu e}+19\left(\tilde{S}_{e\mu}-\tilde{S}^*_{\mu e}\right)|^2\right.\\
&\quad \left.+\,|\tilde{A}_{e\mu}+\tilde{A}^*_{\mu e}-19\left(\tilde{P}_{e\mu}+\tilde{P}^*_{\mu e}\right)|^2\right]\times 10^{-1}\left(\frac{1\ \mathrm{TeV}^4}{\Lambda_{NP}}\right)^4 < 4.7\times 10^{-12}\\
\mathcal{B}\left(K^+ \to \pi^+ e^- \mu^+\right) &= 8.7\left[|V_{\mu e}|^2+|A_{\mu e}|^2+10\left(|S_{\mu e}|^2+|P_{\mu e}|^2\right)\right.\\
&\quad \left.+\ 3.6\ \mathrm{Re}\left(A^*_{\mu e}P_{\mu e}+V^*_{\mu e}S_{\mu e}\right)\right]\times 10^{-2}\left(\frac{1\ \mathrm{TeV}^4}{\Lambda_{NP}}\right)^4 < 1.3\times 10^{-11}. \qquad (21)
\end{aligned}$$

For the last two branching ratios (kaon modes) we have also quoted the current 90% c.l. experimental upper bound. The colour coding suggests how the different modes are complementary being sensitive to different currents (densities). For example, the kaon limits on parity odd quark bilinears are much better than those on the parity even ones whereas the hyperons are sensitive to both. The rates for Ω decays can be similarly obtained and are quoted in [10]. The sensitivity of the different hyperon decay modes is compared in Figure 4. That figure shows that the hyperon modes most

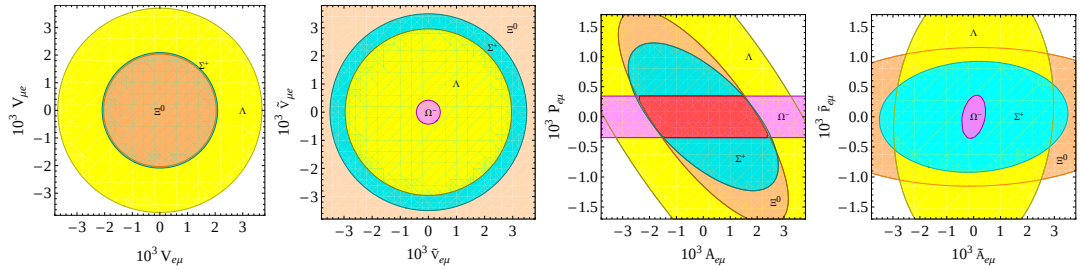

Figure 4: Possible constraints for different hyperon modes, $\Lambda \to ne^-\mu^+$, $\Sigma^+ \to pe^-\mu^+$, $\Xi^0 \to \Lambda e^-\mu^+$, $\Omega^- \to \Xi^- e^-\mu^+$. For these plots we have taken $\Lambda_{NP} = 1$ TeV and assumed that all branching ratios are probed at the 10^{-10} level.

sensitive to NP are those that involve Ω decay. In Figure 5 we compare current kaon constraints to those that can be achieved with a 10^{-12} sensitivity to the Ω branching ratios.

5. $|\Delta S| = 2$ hyperon decay

Within the SM, the short distance $|\Delta S| = 2$ interactions responsible for $K - \bar{K}$ mixing arise from box diagrams that lead to the effective Hamiltonian

$$\mathcal{H}^{SM}_{\Delta S=2} = \frac{\eta_{cc} G_F^2 m_c^2}{4\pi^2}\left(V^*_{cd}V_{cs}\right)^2 \bar{d}\gamma^\alpha P_L s\ \bar{d}\gamma_\alpha P_L s. \qquad (22)$$

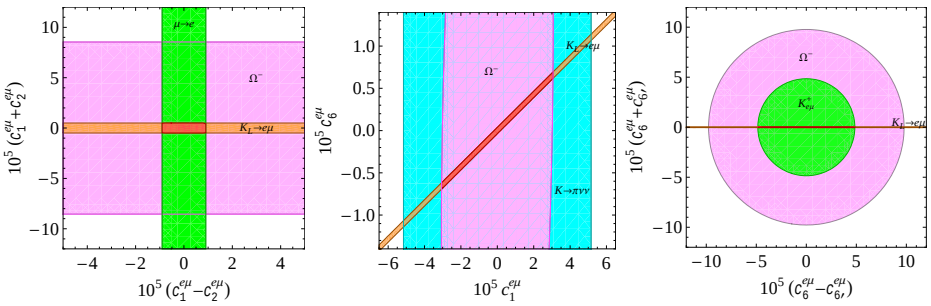

Figure 5: Current constraints placed by $K_L \to e^\pm\mu^\mp, K^+ \to \pi^+e^-\mu^+$ and $\mu \to e$ conversion compared to what can be achieved with a sensitivity of 10^{-12} to $\mathcal{B}(\Omega^- \to \Xi^- e^-\mu^+)$.

The SM prediction that follows, agrees well with the measured kaon mixing and results in tiny hyperon decay rates as we show below. Going beyond the SM, however, we note that the kaon matrix element is only sensitive to parity even operators, whereas the hyperon decay matrix elements are sensitive to both parity even and odd operators and can therefore close the remaining window for new physics in parameter space. This is illustrated schematically in Figure 6

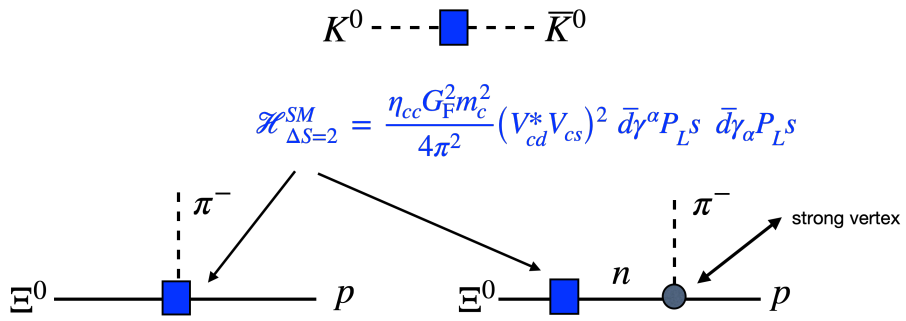

Figure 6: The kaon mixing matrix element (above) is only sensitive to the parity even part of $\mathcal{H}^{SM}_{\Delta S=2}$. The hyperon decay is sensitive to the parity odd part as well as depicted on the lower panel.

To estimate the rates for $|\Delta S| = 2$ hyperon decay within the SM we need to deal with both short and long-distance contributions. For the short-distance contribution, we need to compute the matrix element of Eq. 22. This can be partially achieved by noticing that this operator is part of the same $(27_L, 1_R)$ responsible for the $\Delta I = 3/2$ non-leptonic hyperon decay amplitudes and can thus be related to those rates [34, 35]. When the decuplet is included, there are two low-energy constants in the lowest order in baryon χPT representation of the relevant operator:

$$\begin{aligned}
Q_{LL} &= \bar{d}\gamma^\alpha P_L s\,\bar{d}\gamma_\alpha P_L s = t_{kl,no}\,\overline{\psi}_k\gamma^\alpha P_L\psi_n\,\overline{\psi}_l\gamma_\alpha P_L\psi_o \\
&\to \Lambda_\chi f_\pi^2\, t_{kl,no}\left[\hat{\beta}_{27}\left(\xi\overline{B}\xi^\dagger\right)_{nk}\left(\xi B\xi^\dagger\right)_{ol} + \hat{\delta}_{27}\,\xi_{nx}\xi_{oz}\xi^\dagger_{vk}\xi^\dagger_{wl}\left(\overline{T}_{rvw}\right)^\alpha (T_{rxz})_\alpha\right] \\
\mathcal{H}^{sm}_{\Delta I=3/2,\Delta S=1} &= \sqrt{8}(\hat{c}_1+\hat{c}_2)G_F V_{ud}^* V_{us} Q^{\Delta I=3/2}_{\Delta S=1}, \qquad Q^{\Delta I=3/2}_{\Delta S=1} = \tilde{t}_{kl,no}\overline{\psi}_k\gamma^\alpha P_L\psi_n\overline{\psi}_l\gamma_\alpha P_L\psi_o \\
Q^{\Delta I=3/2}_{\Delta S=1} &\to \Lambda_\chi f_\pi^2\tilde{t}_{kl,no}\left[\hat{\beta}_{27}\left(\xi\overline{B}\xi^\dagger\right)_{nk}\left(\xi B\xi^\dagger\right)_{ol} + \hat{\delta}_{27}\xi_{nx}\xi_{oz}\xi^\dagger_{vk}\xi^\dagger_{wl}\left(\overline{T}_{rvw}\right)^\eta (T_{rxz})_\eta\right] \quad (23)
\end{aligned}$$

In practice, extracting the low energy constant $\hat{\beta}_{27}$ from a fit to $\Delta I = 3/2$ amplitudes is difficult because these represent a tiny fraction of the overall amplitudes (the $\Delta I = 1/2$ rule). The situation

is slightly better for the S-wave of $\Sigma^+ \to n\pi^+$ where the octet matrix element vanishes at leading order in χPT. Using this decay mode we obtain $\hat{\beta}_{27} = 0.076 \pm 0.015$ [12], but cannot fix $\hat{\delta}_{27}$ from data. For numerical estimates, we assume that they are of a similar magnitude.

The $|\Delta S| = 2$ hyperon decay rates that result from this short-distance contribution in the SM are very small as can be seen in Table 2, or Figure 7. Figure 7 illustrates the correlation between two $|\Delta S| = 2$ hyperon modes and ΔM_K taking into account the uncertainty in all the parameters that enter the calculation [12], with the largest uncertainty that appears in the perturbative part of the result being that in $\eta_{cc} = 1.87 \pm 0.76$ [36]. The blue region in the figure marks the experimental value of ΔM_K. The figure illustrates how the SM can accommodate the measured mixing, but it leaves room for NP contributions. It also shows, however, that any short-distance contribution from NP will lead to unobservably small hyperon rates. Following the discussion leading to Figure 6, we can see that the hyperon decay can test NP physics contributions only if they are mostly parity-violating, hence not contributing to kaon mixing. To estimate the effect of long-distance contributions, we

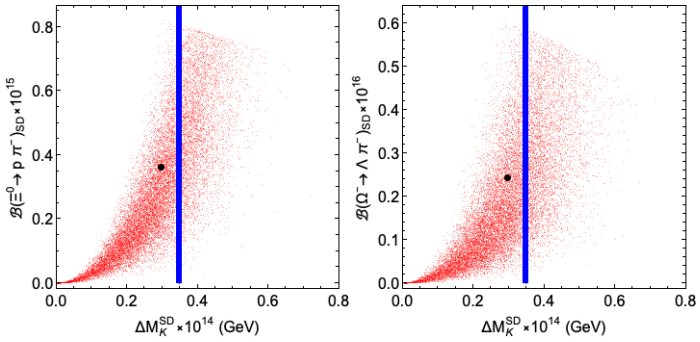

Figure 7: Correlation between $\Xi^0 \to p\pi^-$ and ΔM_K from short distance contributions in the SM, left panel. The same for $\Omega^- \to \Lambda\pi^-$ in the right panel.

need to evaluate pole diagrams such as those sketched in Figure 8. We emphasize, however, that the uncertainty in this estimate is large with the prediction being only an order of magnitude estimate. It

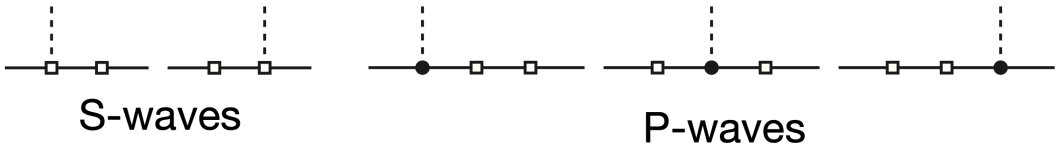

Figure 8: S and P wave pole diagrams to obtain the leading long-distance contributions to $|\Delta S| = 2$ hyperon decays. The open squares represent $|\Delta S| = 1$ weak transitions from Eq. 10 and the solid circle a strong vertex from Eq. 3

.

turns out that the long-distance contributions to these decays are several orders of magnitude larger than their short-distance counterparts, but still below current experimental sensitivity. The left panel of Figure 9 illustrates the dominance of long-distance contributions for the mode $\Omega^- \to nK^-$. The right panel shows an example of correlations between two hyperon modes including both short and long distance terms within the SM. As before, the spread in these scatter plots corresponds to a variation of all parameters within their uncertainties as discussed in [12]. Some of the rates

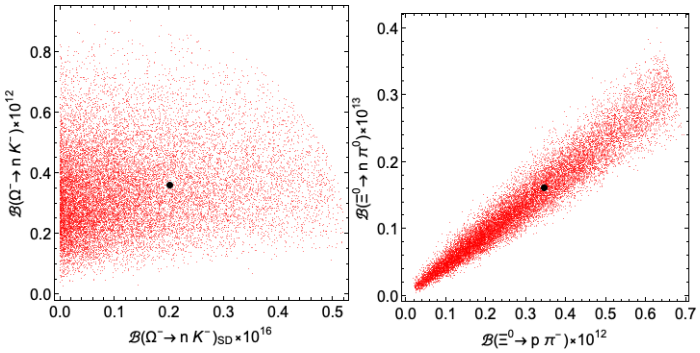

Figure 9: $\Omega^- \to nK^-$ with all contributions vs only short distance contributions (left panel). Correlation between two $|\Delta S| = 2$ hyperon decay modes including both short and long-distance contributions.

we obtained in [12] are tabulated in Table 2. For comparison, the last column also shows the current 90% confidence level upper limit from either HyperCP [37] or BESIII [1]. We now turn our attention to the possibility of constraining new physics, and begin from the effective dimension six four-quark operator,

$$\begin{aligned} \mathcal{H} &= C_{LL}Q_{LL} + C_{RR}Q_{RR} + C_{LR}Q_{LR} + C'_{LR}Q'_{LR} \\ Q_{LL} &= \overline{d}\gamma^\alpha P_L s\,\overline{d}\gamma_\alpha P_L s, \quad Q_{RR} = \overline{d}\gamma^\alpha P_R s\,\overline{d}\gamma_\alpha P_R s \\ Q_{LR} &= \overline{d}\gamma^\alpha P_L s\,\overline{d}\gamma_\alpha P_R s, \quad Q'_{LR} = \overline{d}P_L s\,\overline{d}P_R s \end{aligned} \tag{24}$$

In this effective Hamiltonian, the term Q_{LL} is the one that occurs in the SM whereas Q_{RR} and Q_{LR} occur in left-right models and Q'_{LR} is induced by renormalization. With these four operators, it is possible to represent NP with Wilson coefficients such that kaon mixing is suppressed but $|\Delta S| = 2$ hyperon decay rates are not. There are several options, for example, the Wilson coefficients can be fine-tuned relying on the fact that $Q_{LL,RR}$ have a different kaon matrix element than Q'_{LR}[12]. A second possibility is to find models where the Wilson coefficients satisfy $C_{LL} = -C_{RR}$, resulting in a parity odd operator that does not contribute to kaon mixing [34]. One example discussed in [12]

Mode	$\mathcal{B}_{SD}$	$\mathcal{B}_s$	90% c.l. limit
$\Xi^0 \to p\pi^-$	$(0.03, 1) \times 10^{-15}$	$(0.01, 2.6) \times 10^{-14}$	8×10^{-6} [37]
$\Xi^0 \to n\pi^0$	$(0.03, 1) \times 10^{-15}$	$(0., 0.9) \times 10^{-15}$	
$\Xi^- \to n\pi^-$	$(0.07, 2.6) \times 10^{-16}$	$(0.01, 1.3) \times 10^{-14}$	1.5×10^{-5}[37]
$\Omega^- \to nK^-$	$(0.1, 6.5) \times 10^{-17}$	$(0.2, 0.6) \times 10^{-12}$	2.4×10^{-4} [1]
$\Omega^- \to \Lambda\pi^-$	$(0.2, 7.1) \times 10^{-17}$	$(0.4, 1.5) \times 10^{-13}$	2.9×10^{-6} [37]
$\Omega^- \to \Sigma^0\pi^-$	$(0.04, 1.7) \times 10^{-17}$	$(0.5, 3.1) \times 10^{-14}$	5.4×10^{-4} [1]

Table 2: 90%-CL intervals of branching fractions of selected $\Delta S = 2$ hyperon decays in the SM from the short-distance contribution only (second column), and complete contributions with h_D, h_F, h_C parameters obtained from a fit to the s-waves (third column)[12]. The last column quotes 90% c.l. upper limits when available.

consists of a Z' with flavour changing neutral couplings $\mathcal{L}_{dsZ'} = -\bar{d}\gamma^\beta \left(g_L P_L + g_R P_R\right) s\, Z'_\beta$, which after QCD corrections gives the following contribution to kaon mixing

$$\Delta M_K^{Z'} = \frac{2}{4 m_{K^0} m_{Z'}^2} \Re \left(\eta_{LL} \left(g_L^2 + g_R^2\right) \langle Q_{LL} \rangle + 2 g_L g_R \left(\eta_{LR} \langle Q_{LR} \rangle + \eta'_{LR} \langle Q'_{LR} \rangle \right) \right) \tag{25}$$

The last two terms in this expression are negative (the lattice matrix element $\langle Q_{LR} \rangle$ as well as η'_{LR} are both negative) whereas the first two are positive. Allowing $-1 < \Delta M_K^{Z'} / \Delta M_K^{\rm exp} < 0.5$ which is within the 2σ range of the measurement, and taking that $g_{L,R}$ to be real, we show in Figure 10 regions of parameter space where $\mathcal{B}(\Xi^0 \to p\pi^-)$ can be large.

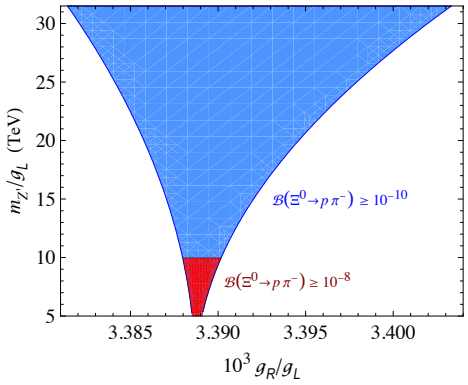

Figure 10: Couplings in Eq. 25 where ΔM_K remains within 2σ of its measured value but $\mathcal{B}(\Xi^0 \to p\pi^-)$ can be large.

6. Summary and Conclusions

Hyperon decay can play a role in probing physics beyond the standard model in the $s \to d$ sector complementing the reach of kaon physics. To significantly probe new physics possibilities much higher sensitivities are needed than currently available. In the near future, LHCb can rule out the "hyperCP" particle and provide a good measurement of the dimuon mass distribution in $\Sigma^+ \to p\mu^+\mu^-$. That result can be used for both improvement of our understanding of form factors and for exotic particle searches. A more precise measurement of the rate, combined with new measurements of $\Sigma^+ \to pe^+e^-$ and $\Sigma^+ \to p\gamma$ can pinpoint the SM prediction and improve constraints on NP for directions in parameter space where the kaons are not sensitive. Expected future sensitivity at the LHCb experiment can provide similar constraints for the $\Delta S = 2$ NP parameter space and begin to probe exotic scenarios. The BESIII hyperon program can also improve measurements in many of these modes.

Acknowledgments

This work was supported in part by the Australian Government through the Australian Research Council. This talk was based on work done in collaboration with Xiao-Gang He and Jusak Tandean.

References

[1] BESIII collaboration, M. Ablikim et al., *Search for $\Delta S = 2$ nonleptonic hyperon decays $\Omega^- \to \Sigma^0\pi^-$ and $\Omega^- \to nK^-$*, 2403.13437.

[2] BESIII collaboration, M. Ablikim et al., *Precision Measurement of the Decay $\Sigma^+ \to p\gamma$ in the Process $J/\psi \to \Sigma^+\Sigma^-$*, *Phys. Rev. Lett.* **130** (2023) 211901, [2302.13568].

[3] LHCb collaboration, R. Aaij et al., *Evidence for the rare decay $\Sigma^+ \to p\mu^+\mu^-$*, *Phys. Rev. Lett.* **120** (2018) 221803, [1712.08606].

[4] A. A. Alves Junior et al., *Prospects for Measurements with Strange Hadrons at LHCb*, *JHEP* **05** (2019) 048, [1808.03477].

[5] G. Anzivino et al., *Workshop summary – Kaons@CERN 2023*, 2311.02923.

[6] BESIII collaboration, M. Ablikim et al., *Future Physics Programme of BESIII*, *Chin. Phys. C* **44** (2020) 040001, [1912.05983].

[7] M. Achasov et al., *STCF conceptual design report (Volume 1): Physics & detector*, *Front. Phys. (Beijing)* **19** (2024) 14701, [2303.15790].

[8] E. E. Jenkins and A. V. Manohar, *Chiral corrections to the baryon axial currents*, *Phys. Lett. B* **259** (1991) 353–358.

[9] X.-G. He, J. Tandean and G. Valencia, *Implications of a new particle from the hyperCP data on $\Sigma^+ \to p\mu^+\mu^-$*, *Phys. Lett. B* **631** (2005) 100–108, [hep-ph/0509041].

[10] X.-G. He, J. Tandean and G. Valencia, *Charged-lepton-flavor violation in $|\Delta S| = 1$ hyperon decays*, *JHEP* **07** (2019) 022, [1903.01242].

[11] Particle Data Group collaboration, R. L. Workman and Others, *Review of Particle Physics*, *PTEP* **2022** (2022) 083C01.

[12] X.-G. He, J. Tandean and G. Valencia, *$\Delta S = 2$ nonleptonic hyperon decays as probes of new physics*, *Phys. Rev. D* **108** (2023) 055012, [2304.02559].

[13] E. E. Jenkins and A. V. Manohar, *Baryon chiral perturbation theory using a heavy fermion Lagrangian*, *Phys. Lett. B* **255** (1991) 558–562.

[14] NA48/I collaboration, J. R. Batley et al., *Measurement of the branching ratios of the decays $\Xi^0 \to \Sigma^+ e^- \bar{\nu}_e$ and $\bar{\Xi}^0 \to \bar{\Sigma}^+ e^+ nu_e$*, *Phys. Lett. B* **645** (2007) 36–46, [hep-ex/0612043].

[15] HyperCP collaboration, H. Park et al., *Evidence for the Decay $\Sigma^+ \to p\mu^+\mu^-$*, *Phys. Rev. Lett.* **94** (2005) 021801, [hep-ex/0501014].

[16] X.-G. He, J. Tandean and G. Valencia, *The decay $\Sigma^+ \to p\ell^+\ell^-$ within the standard model*, *Phys. Rev. D* **72** (2005) 074003, [hep-ph/0506067].

[17] H. Neufeld, *Weak radiative baryon decays in chiral perturbation theory*, *Nucl. Phys. B* **402** (1993) 166–194.

[18] E. E. Jenkins, M. E. Luke, A. V. Manohar and M. J. Savage, *Weak radiative hyperon decays in chiral perturbation theory*, *Nucl. Phys. B* **397** (1993) 84–104, [hep-ph/9210265].

[19] J. W. Bos, D. Chang, S. C. Lee, Y. C. Lin and H. H. Shih, *Hyperon weak radiative decays in chiral perturbation theory*, *Phys. Rev. D* **54** (1996) 3321–3328, [hep-ph/9601299].

[20] J. W. Bos, D. Chang, S. C. Lee, Y. C. Lin and H. H. Shih, *Heavy baryon chiral perturbation theory and reparametrization invariance*, *Phys. Rev. D* **57** (1998) 4101–4107, [hep-ph/9611260].

[21] X.-G. He, J. Tandean and G. Valencia, *Decay rate and asymmetries of* $\Sigma^+ \to p\mu^+\mu^-$, *JHEP* **10** (2018) 040, [1806.08350].

[22] R.-X. Shi, S.-Y. Li, J.-X. Lu and L.-S. Geng, *Weak radiative hyperon decays in covariant baryon chiral perturbation theory*, *Sci. Bull.* **67** (2022) 2298–2304, [2206.11773].

[23] A. Roy, J. Tandean and G. Valencia, *The decays* $\Sigma^+ \to p\ell^+\ell^-$ *within the standard model and beyond*, 2404.15268.

[24] F. Erben, V. Gulpers, M. T. Hansen, R. Hodgson and A. Portelli, *Prospects for a lattice calculation of the rare decay* $\Sigma^+ \to p\ell^+\ell^-$, *JHEP* **04** (2023) 108, [2209.15460].

[25] V. Chobanova, G. D'Ambrosio, T. Kitahara, M. Lucio Martinez, D. Martinez Santos, I. S. Fernandez et al., *Probing SUSY effects in* $K_S^0 \to \mu^+\mu^-$, *JHEP* **05** (2018) 024, [1711.11030].

[26] S. Neshatpour and F. Mahmoudi, *Flavour Physics Phenomenology with SuperIso*, *PoS* **CompTools2021** (2022) 010, [2207.04956].

[27] G. Buchalla, G. D'Ambrosio and G. Isidori, *Extracting short distance physics from* $K_{(L,S)} \to \pi^0 e^+ e^-$ *decays*, *Nucl. Phys. B* **672** (2003) 387–408, [hep-ph/0308008].

[28] G. Isidori, C. Smith and R. Unterdorfer, *The Rare decay* $K_L \to \pi^0\mu^+\mu^-$ *within the SM*, *Eur. Phys. J. C* **36** (2004) 57–66, [hep-ph/0404127].

[29] F. Mescia, C. Smith and S. Trine, $K_L \to \pi^0 e^+ e^-$ *and* $K_L \to \pi^0\mu^+\mu^-$*: a binary star on the stage of flavor physics*, *JHEP* **08** (2006) 088, [hep-ph/0606081].

[30] G. D'Ambrosio, A. M. Iyer, F. Mahmoudi and S. Neshatpour, *Anatomy of kaon decays and prospects for lepton flavour universality violation*, *JHEP* **09** (2022) 148, [2206.14748].

[31] J. Tandean and G. Valencia, *CP violation in hyperon nonleptonic decays within the standard model*, *Phys. Rev. D* **67** (2003) 056001, [hep-ph/0211165].

[32] P. Mertens and C. Smith, *The* $s \to d\gamma$ *decay in and beyond the Standard Model*, *JHEP* **08** (2011) 069, [1103.5992].

[33] L.-S. Geng, J. M. Camalich and R.-X. Shi, *New physics in $s \to d$ semileptonic transitions: rare hyperon vs. kaon decays*, *JHEP* **02** (2022) 178, [2112.11979].

[34] X.-G. He and G. Valencia, *$\Delta I = 3/2$ and $\Delta S = 2$ hyperon decays in chiral perturbation theory*, *Phys. Lett. B* **409** (1997) 469–473, [hep-ph/9705462].

[35] A. Abd El-Hady, J. Tandean and G. Valencia, *Chiral perturbation theory for $|\Delta I| = 3/2$ hyperon decays*, *Nucl. Phys. A* **651** (1999) 71–89, [hep-ph/9808322].

[36] J. Brod and M. Gorbahn, *Next-to-Next-to-Leading-Order Charm-Quark Contribution to the CP Violation Parameter ϵ_K and ΔM_K*, *Phys. Rev. Lett.* **108** (2012) 121801, [1108.2036].

[37] HyperCP collaboration, C. G. White et al., *Search for $\Delta S = 2$ nonleptonic hyperon decays*, *Phys. Rev. Lett.* **94** (2005) 101804, [hep-ex/0503036].